



저작자표시-변경금지 2.0 대한민국

이용자는 아래의 조건을 따르는 경우에 한하여 자유롭게

- 이 저작물을 복제, 배포, 전송, 전시, 공연 및 방송할 수 있습니다.
- 이 저작물을 영리 목적으로 이용할 수 있습니다.

다음과 같은 조건을 따라야 합니다:



저작자표시. 귀하는 원저작자를 표시하여야 합니다.



변경금지. 귀하는 이 저작물을 개작, 변형 또는 가공할 수 없습니다.

- 귀하는, 이 저작물의 재이용이나 배포의 경우, 이 저작물에 적용된 이용허락조건을 명확하게 나타내어야 합니다.
- 저작권자로부터 별도의 허가를 받으면 이러한 조건들은 적용되지 않습니다.

저작권법에 따른 이용자의 권리는 위의 내용에 의하여 영향을 받지 않습니다.

이것은 [이용허락규약\(Legal Code\)](#)을 이해하기 쉽게 요약한 것입니다.

[Disclaimer](#)

의학박사 학위논문

# **Inhibition Effects of Adiponectin- based Peptide and Dasatinib in Keloids**

아디포넥틴 유래의 펩타이드와 다사티닙의  
켈로이드 억제효과

2020 년 7 월

서울대학교 대학원

의학과 피부과학전공

**Claudia Christin Darmawan**

# **Inhibition Effects of Adiponectin- based Peptide and Dasatinib in Keloids**

지도교수 문제호

이 논문을 의학박사 학위논문으로 제출함

2020 년 7 월

서울대학교 대학원

의학과 피부과학전공

**Claudia Christin Darmawan**

클라우디아의 박사 학위논문을 인준함

2020 년 7 월

위 원 장 \_\_\_\_\_ (인)

부 위 원 장 \_\_\_\_\_ (인)

위 원 \_\_\_\_\_ (인)

위 원 \_\_\_\_\_ (인)

위 원 \_\_\_\_\_ (인)

# **Inhibition Effects of Adiponectin- based Peptide and Dasatinib in Keloids**

by  
Claudia Christin Darmawan  
(Directed by Je-ho Mun, M.D., Ph.D.)

A thesis submitted to the Department of Medicine in partial fulfillment of  
the requirements for the degree of Doctor of Philosophy in Medicine  
(Dermatology) at Seoul National University College of Medicine

**July, 2020**

**Approved by thesis committee**

Professor \_\_\_\_\_ Chairman  
Professor \_\_\_\_\_ Vice chairman  
Professor \_\_\_\_\_  
Professor \_\_\_\_\_  
Professor \_\_\_\_\_

**Contents**

ABSTRACT \_\_\_\_\_ 1

LIST OF TABLES	3
LIST OF FIGURES	4
ABBREVIATIONS	5
INTRODUCTION	6
CHAPTER 1	
BACKGROUND	8
MATERIALS AND METHODS	9
RESULTS	14
DISCUSSION	24
CHAPTER 2	
BACKGROUND	28
MATERIALS AND METHODS	29
RESULTS	34
DISCUSSION	41
REFERENCES	44
ABSTRACT IN KOREAN	48

## **Abstract**

# **Inhibition Effects of Adiponectin-based Peptide and Dasatinib in Keloids**

**Claudia Christin Darmawan**

Department of Dermatology, College of Medicine,  
The Graduate School Seoul National University

Keloid is a benign cutaneous overgrowth of dermal fibroblasts that are caused by pathologic scarring on wound healing. It may occur after an apparent injury to the skin tissue, but may develop up to several years after minor injuries, or even spontaneously without any perceivable injuries. It persists for a long period of time and does not regress spontaneously. This lesion may significantly affect patient's quality of life, both physically and psychologically. Their complex pathogenesis is not clearly elucidated up to date and various current surgical and therapeutic modalities are still unsatisfactory.

In chapter 1, we investigated the effect of adiponectin-based short peptide on TGF- $\beta$ 1 induced fibrosis in keloid. The effect of adiponectin peptide on TGF- $\beta$ 1 induced fibrosis were evaluated using primary culture of keloid fibroblast. Keloid tissues were xenotransplanted to the back of athymic nude mice to investigate the effect of intralesional injection of adiponectin peptide on keloid lesion. Adiponectin peptide significantly attenuated the TGF- $\beta$ 1 induced procollagen type 1 expression in keloid fibroblasts ( $p < 0.05$ ). It inhibited the TGF- $\beta$ 1 induced phosphorylation of SMAD3 and ERK while it amplified the phosphorylation of AMPK ( $p < 0.05$ ). Knockdown of Adiponectin Receptor 1 (AdipoR1) reversed the attenuation of procollagen expression on adiponectin peptide treated TGF- $\beta$ 1 induced fibrosis ( $p < 0.05$ ). Treatment with adiponectin peptide significantly reduced the gross weight and procollagen expression of

keloid tissues than those in the control in the xenograft mice.

In chapter 2, we investigated the presence of senescent fibroblasts in keloid cells and to assess the senolytic effect of dasatinib in keloid fibroblasts. Senescence-associated  $\beta$ -galactosidase positive cells and p16-expressing cells were higher in keloid lesional fibroblasts compared to those in perilesional normal fibroblasts ( $p < 0.05$ ). Dasatinib induced selective death of senescent cell and decreased the expression of procollagen in cultured keloid fibroblasts. Xenotransplantation model using athymic nude mice with implanted keloid tissues showed that intralesional injection of dasatinib reduced the gross weight and suppressed the level of procollagen and p16 expression in keloid tissues.

In summary, the results of this study showed a possible therapeutic application of adiponectin peptide and dasatinib for keloid treatment.

**Keywords** : Keloid, Scar, Adiponectin, Peptide, Treatment,  
Senescent, Senolytics, Dasatinib

**Student Number** : 2017-23763

## **LIST OF TABLES**

Table 1. Primer sequences for qRT-PCR (chapter 1)

Table 2. Primer sequences for qRT-PCR (chapter 2)

Table 3. Skin diseases associated with cellular senescence

## LIST OF FIGURES

- Figure 1. Effect of ADP355 on keloid fibroblast viability and the AMP-activated protein kinase (AMPK) pathway.
- Figure 2. Effect of ADP355 on keloid and normal fibroblast
- Figure 3. Effect of ADP355 on TGF- $\beta$ 1-induced procollagen expression.
- Figure 4. Effect of ADP355 on the TGF- $\beta$ 1-induced downstream pathways.
- Figure 5. Knockdown of adiponectin receptor 1 (AdipoR1) reversed the ADP355 at tenuation of TGF- $\beta$ 1-induced collagen expression.
- Figure 6. Intralesional Injection of ADP355 Reduced the Size and Procollagen Expression of Xenotransplanted Keloid Tissue.
- Figure 7.  $\beta$ -galactosidase activity analysis on primary cultured fibroblast of keloid patients.
- Figure 8. Expression of p16 in keloid lesion
- Figure 9. Effect of dasatinib on cultured keloid fibroblasts.
- Figure 10. The effect of dasatinib on xenotransplantation model of keloid.
- Figure 11. Histopathological analysis of intralesional Dasatinib on xenotransplantation model of keloid.

## ABBREVIATIONS

AdipoQ	Adiponectin recombinant protein
AdipoR	Adiponectin receptor
ADP355	Adiponectin 355
AMPK	AMP-activated protein kinase
ECM	Extracellular matrix
ERK	Extracellular signal-regulated kinase
IPF	Idiopathic pulmonary fibrosis
p-AMPK	Phosphorylation AMP-activated protein kinase
p-ERK	Phosphorylated extracellular signal-regulated kinase
p-AMPK	Phosphorylated AMP-activated protein kinase
SASP	Senescence-associated secretory phenotype
siRNA	Small interfering RNA
t-AMPK	Total AMP-activated protein kinase
TGF- $\beta$	Transforming growth factor beta

## INTRODUCTION

Keloids are a type of excessive scarring, which results from aberrations in physiologic wound healing. They generally occur after apparent injury to the skin tissue such as trauma, surgery, acne burn or ear-piercing <sup>1</sup>. Factors such as genetic predisposition is suggested due to higher incidence in darker skin individuals and Asian with more familial aggregation <sup>2,3</sup>. Keloids persist for long periods and do not regress spontaneously <sup>1</sup>. This condition is characterized by benign cutaneous hyperproliferation of dermal fibroblasts, overproduction of collagen, fibronectin and other extracellular matrix components, and increased infiltration of inflammatory cells with high recurrence rates <sup>4,5</sup>. Symptoms such as itching, pain and cosmetic deformities, can significantly affect the patient's quality of life, both physically and psychologically <sup>6</sup>.

Appropriate management of keloids is therefore necessary. Several available treatment modalities such as surgical excision, intralesional corticosteroid injection, 5-fluorouracil, pressure therapy, silicone gel sheets, and pulsed-dye laser are available. However, these methods often do not have a satisfactory outcome and impose a discernable rate of recurrence <sup>7</sup>.

Therefore, given the limitation of current therapeutic modalities in keloid, we performed an investigation on the effect adiponectin-based peptide and dasatinib (as a senolytic drug) in keloids.

## **CHAPTER 1**

# **Adiponectin-Based Peptide Inhibits Transforming Growth Factor- $\beta$ 1-induced Fibrosis in Keloids**

## BACKGROUND

Adiponectin, an adipokine that is predominantly secreted by adipose tissue, exerts its multifunctional effect through interactions with cell-surface adiponectin receptors (AdipoRs)<sup>8,9</sup>. Adiponectin elicits several downstream signaling events. APPL1 (adaptor protein containing pleckstrin homology domain, phosphotyrosine binding domain, and leucine zipper motif) mediates the intracellular signal transduction of the adiponectin receptor pathway. It activates AMP activated protein kinases (AMPK), PPAR- $\alpha$ , calcium/calmodulin-dependent protein kinase kinase (CaMKK- $\beta$ ), and p38 MAPK.<sup>10,11</sup> Adiponectin has distinct target tissue specificity and modulates unique biological processes; it improves insulin sensitivity, regulates energy metabolism, and modulates the inflammatory response<sup>12</sup>.

A recent study has shown that adiponectin attenuates connective tissue growth factor-induced keloid fibrosis, migration, and extracellular matrix (ECM) overproduction<sup>13</sup>. These findings indicate a possible novel role of adiponectin in keloid treatment. However, adiponectin is a relatively large (244 amino acids) cytokine<sup>14</sup>. In 2011, an adiponectin-based short peptide, named ADP355 (H-DAsn-Ile-Pro-Nva-Leu-Tyr-DSer-Phe-Ala-DSer-NH<sub>2</sub>), that can mimic adiponectin action was developed as a suitable drug for preclinical and clinical development<sup>8</sup>. Previous studies have shown that ADP355 has an anti-fibrotic effect on liver fibrosis and systemic sclerosis<sup>15-17</sup>.

Therefore, in this study, we investigated the effect of ADP355 in keloid fibroblasts and xenograft mice to determine the therapeutic benefits of adiponectin peptide for the treatment of keloids.

## **MATERIALS AND METHODS**

### **Ethics statement**

The study protocols were approved by the institutional research board of Seoul National University Hospital (IRB No. C-1711-070-899), and written informed consent was obtained from all subjects. All experimental procedures using human tissues were conducted according to the principles described in the Declaration of Helsinki. The animal study was approved by the Institutional Animal Care and Use Committee (IACUC) at Seoul National University Hospital (IACUC No. 18-0261-S1A0) and all the methods were performed in accordance with the relevant guidelines and regulations.

### **Isolation of keloid and keloid dermal fibroblast primary cell culture**

Keloid tissues were obtained from seven patients during keloid removal surgery (Supplementary Figures 1). Patients with keloids were all diagnosed by pathological examination. No patients received any treatment six months prior to surgery. Human dermal fibroblasts were isolated by mechanical and enzymatic digestion using a previously described protocol<sup>18</sup>. Cells were cultured in Dulbecco's modified Eagle's medium (DMEM) purchased from Welgene (Gyeongsan, South Korea) with penicillin (400 U/ml) and streptomycin (50 mg/ml) purchased from Life Technologies (Rockville, MD), and 10% FBS in a humidified 5% CO<sub>2</sub> atmosphere at 37 °C. Keloid fibroblasts between passage 1 and 4 were used for the subsequent experiments.

### **Adiponectin peptide treatment**

ADP355 (H-D<sub>Asn</sub>-Ile-Pro-Nva-Leu-Tyr-D<sub>Ser</sub>-Phe-Ala-D<sub>Ser</sub>-NH<sub>2</sub>) was purchased from Pepton (Daejeon, South Korea). Cells were seeded on a 6-well plate

in duplicate, and upon reaching 80-90% confluence, cells were starved in serum-free medium for 24 h. Cells were treated with TGF- $\beta$  and ADP355 or AdipoQ simultaneously, and then harvested 24 h after treatment.

### **Cell viability analysis**

Cells were seeded in a 96-well plate at a density of 1800 cells per well and incubated for 24 h at 37 °C. Cells were cultured to 60% confluence and starved for another 24 h in serum-free DMEM and treated with ADP355 (5–100  $\mu$ g/ml) for 24 h. Cell viability was tested using the Ezy-cytox cell viability assay kit (Daeil Bio, Suwon, South Korea) according to the manufacturer's instructions. Briefly, Ezy-cytox reagent was added to each well and incubated for 1 h. The absorbance of collected medium was determined spectrophotometrically using a microplate reader (Molecular Devices, Sunnyvale, CA) at 450/650 nm.

### **Western blot analysis**

Following the treatment under appropriate conditions for 24 h, cells were harvested, washed with ice-cold PBS, and lysed with radioimmunoprecipitation assay lysis buffer (EMD Millipore, Billerica, MA, USA) mixed with a protease inhibitor mixture (Roche Applied Science, Penzberg, Germany) and a phosphatase inhibitor mixture (Sigma-Aldrich; Merck KGaA). Cell lysates were centrifuged at 13,500 g at 4 °C for 15 min, and the resultant supernatants were collected. The total extract protein was quantified using a bicinchoninic acid assay reagent (Sigma-Aldrich; Merck KGaA). Equal amounts of protein were then separated using 10% sodium dodecyl sulphate polyacrylamide gel electrophoresis and transferred to polyvinylidene difluoride membranes (Roche Applied Science). The membranes were blocked with 5% skim milk diluted in tris-buffered saline containing 0.1% Tween-20, followed by overnight incubation with the target protein primary antibodies— $\beta$ -actin (Santa Cruz, CA, USA), procollagen type-1 (Developmental

studies Hybridoma Bank, IA, USA), p-ERK (Santa Cruz, CA, USA), t-AMPK (Cell Signaling, MA, USA), p-AMPK (Cell Signaling), p-SMAD2 (Santa Cruz), and p-SMAD3 (Santa Cruz).  $\beta$ -actin was used as a loading control. The membranes were washed and incubated with mouse polyclonal antibodies (Genetex, CA, USA) against  $\beta$ -actin and procollagen, and rabbit polyclonal antibodies (Genetex, CA, USA) against p-ERK, p-SMAD2, p-SMAD3, p-AMPK, and t-AMPK. Immunoreactive bands were then visualized using the enhanced chemiluminescence detection system (Thermo Fisher Scientific, MA, USA). Band density was measured using ImageJ software version 1.51w (National Institutes of Health, Bethesda, MD, USA).<sup>19</sup> The protein expression was normalized to that of  $\beta$ -actin.

### siRNA transfection

AdipoR1 in the keloid dermal fibroblasts was depleted through transfection of 100 nM siRNA into the keloid fibroblasts using lipofectamine 2000 (Invitrogen, CA, USA) following the manufacturer's protocol. The existence of siRNA off-target effects was excluded by use of a negative control siRNA. After 18 h of transfection, the cells were treated following the same treatment protocol with/without TGF- $\beta$ 1 and ADP355 or AdipoQ in serum-free DMEM for 24 h. mRNA expression of AdipoR1 was examined by quantitative real-time reverse transcription PCR (RT-PCR). Procollagen expression was examined by western blot analysis using the previously described protocol.

Gene	Forward Primer	Reverse Primer
AdipoR1	CCT GCC AGT	AGG AGA AGC
	AAC AGG GAA	TGA GGC AGA
36B4	TGG GCT CCA	GGC TTC GCT
	AGC AGA TGC	GGC TCC CAC

Table 1. Primer sequences for qRT-PCR

## **Animal model and keloid xenotransplantation**

Keloid tissues were acquired from affected patients during surgical excision. The tissues were cut into small pieces using a 5 mm punch. They were preserved in normal saline and implanted on the backs of female athymic nude BALB/c mice (aged 12 weeks) within 3 h of acquisition. The gross weight of each tissue sample was calculated prior to implantation. The weight of the implanted keloid tissue ranged from 0.07 to 0.1 g (mean, 0.087 g). The mice were anesthetized with isoflurane, and three 5 mm punches were used to make a recipient defect on the back of the mice where the keloids could be transplanted and sutured. Once the wound completely healed and was covered with flesh-colored skin on day 24, the lesions on each mouse were assigned for injection with vehicle (phosphate buffer solution), 10  $\mu$ M adiponectin-based peptide ADP355, or 10  $\mu$ M adiponectin recombinant for six treatments over two weeks. Following this, the lesions were excised to determine the effect of the treatment. This study was approved by The Institutional Animal Care and Use Committee (IACUC) of Seoul National University, and the number of animals used were kept to a minimum in order to reduce their suffering, according to protocol.

## **Tissue analysis**

The tissue samples' gross weights were evaluated. The weights of the grafts after six injections within two weeks were normalized against the weights of the grafts before implantation (mean  $\pm$  standard deviation). The tissue weight reduction in treatment groups was compared to that in the control group. The remaining snap-frozen tissues were lysed with radioimmunoprecipitation assay lysis buffer (EMD Millipore, Billerica, MA, USA) mixed with protease inhibitor mixture (Roche Applied Science, Penzberg, Germany), and western blot analysis was carried out according to the protocol previously described.

## **Statistical analysis**

The results of at least three independent representative experiments with each of the data represented as mean values (SD). A Mann-Whitney U test was used to compare medians between two independent groups and Kruskal-Wallis test was used for comparisons of median values among three or more groups, followed by post-hoc testing using Mann-Whitney U tests with a Bonferroni-adjusted alpha level with SPSS 23.0 software (IBM Co., Armonk, NY, USA) and p values of  $< 0.05$  were considered statistically significant.

## RESULTS

### **Effect of ADP355 on keloid fibroblast viability and the AMP-activated protein kinase (AMPK) pathway**

Firstly, we performed a keloid cell viability test to exclude the possible cytotoxic effect of ADP355 that may indirectly affect the production of procollagen type 1. We investigated the effect of ADP355 on keloid cell viability at 5, 10, 50, and 100 µg/ml. ADP355 did not affect keloid fibroblast viability at doses of 5 to 10 µg/ml, although significantly decreased cell viability was observed at doses ranging from 50 to 100 µg/ml (Figure 1A). Based on these results, further experiments were conducted using an ADP355 dose ranging from 5 to 10 µg/ml. At 10 µg/ml, ADP355 increased the phosphorylation of AMPK in a time-dependent manner, with the most significant activity observed 24 h after treatment of the keloid fibroblasts (Figure 1B). To observe the effect of ADP355 on procollagen expression in keloid fibroblasts and normal fibroblasts, we treated ADP355 ranging from 0.5µg/ml to 10 µg/ml. While the procollagen expression in normal fibroblasts increased, the procollagen expression in keloid fibroblast reduced in concentration dependent manner and showed significant difference at dose of 10µg/ml. (Figure 2).

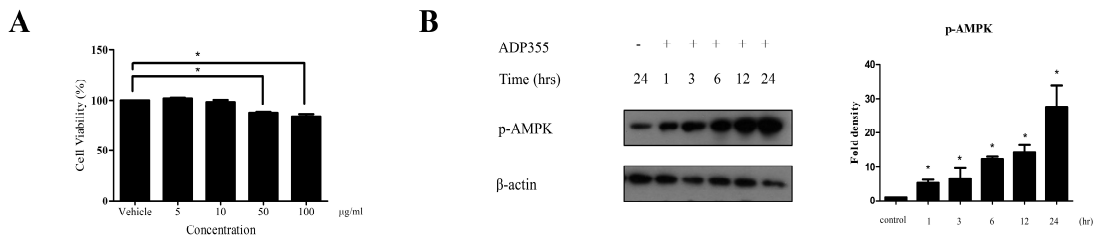


**Figure 1. Effect of ADP355 on keloid fibroblast viability and the AMP-activated protein kinase (AMPK) pathway.**

(A) Viability of keloid fibroblasts was evaluated at ADP355 doses ranging from 5 to 100 µg/ml. ADP355 affected cell viability significantly at doses  $\geq 50$  µg/ml (A,  $p < 0.05$ , cut-off  $> 90\%$ ). (B) At 10 µg/ml, ADP355 increased the activation of the AMP-activated protein kinase (AMPK) pathway in a time-dependent manner from 1 to 24h (B, \*  $p < 0.05$ ). The data are expressed as mean  $\pm$  SD. Representative data are shown from three independent experiments.

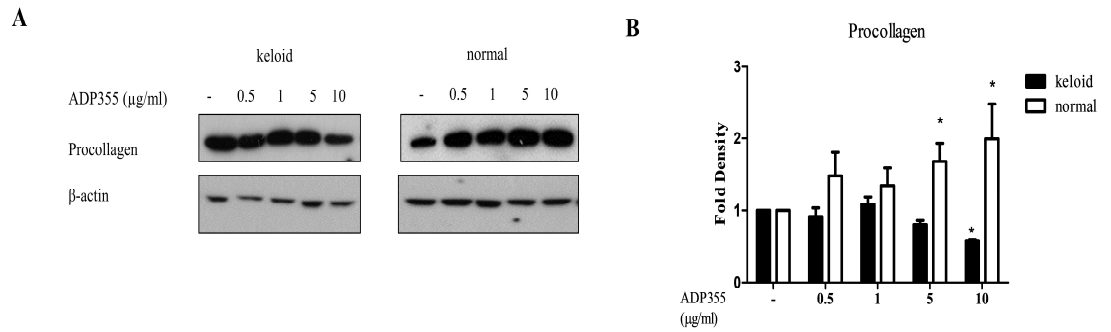


**Figure 2. Effect of ADP355 on keloid fibroblasts and normal fibroblasts.** 10 µg/ml of ADP355 significantly decreased the procollagen expression on keloid fibroblasts while procollagen expression increased in normal fibroblasts at 5µg/ml and 10µg/ml ADP 355. ( $p < 0.05$ ). The data are expressed as mean  $\pm$  SD. Representative data are shown from three independent experiments.

### ADP355 suppressed the production of procollagen type 1 expression

The effect of ADP355 on procollagen expression was investigated in TGF- $\beta$ 1 (5 ng/ml)-induced fibroblasts. TGF- $\beta$ 1 significantly increases procollagen production. However, production was attenuated following treatment with 10  $\mu$ g/ml of ADP355 to levels comparable to those of the positive control of 10  $\mu$ g/ml adiponectin recombinant (AdipoQ). These results suggested that 10  $\mu$ g/ml ADP355 attenuated TGF- $\beta$ 1-induced procollagen type 1 expression in keloid fibroblasts (Figure 3). Subsequent experiments were conducted using a dose of 10  $\mu$ g/ml ADP355.

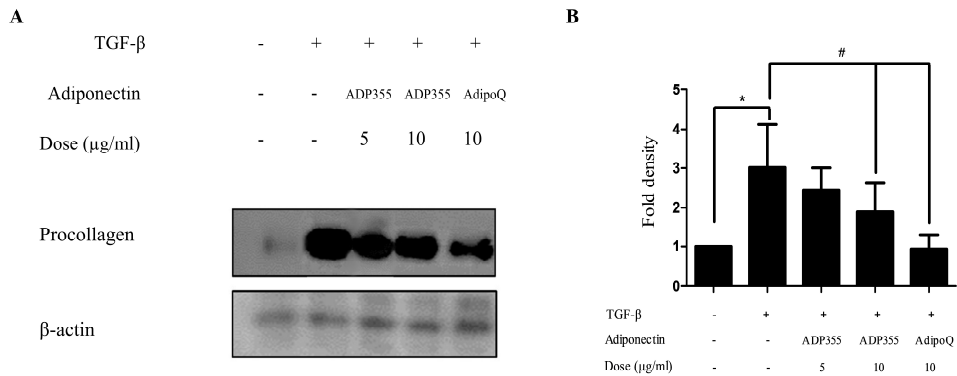


**Figure 3. Effect of ADP355 on TGF- $\beta$ 1-induced procollagen expression.**

(A) Western blot analysis results. Treatment of ADP355 (5 and 10  $\mu$ g/mL) and adiponectin recombinant, AdipoQ (10  $\mu$ g/mL), simultaneously with TGF- $\beta$ 1 10  $\mu$ g/mL of ADP355 and AdipoQ, attenuated TGF- $\beta$ 1-induced procollagen expression. (B) Quantification of western blot results (\*  $p < 0.05$ , control vs. TGF- $\beta$ 1, #  $p < 0.05$ , TGF- $\beta$ 1 vs. TGF- $\beta$ 1 + ADP355, and TGF- $\beta$ 1 vs. TGF- $\beta$ 1 + AdipoQ). The data are expressed as mean  $\pm$  SD. Representative data are shown from three independent experiments.

### **ADP355 Attenuated Phosphorylation of ERK and SMAD3 and Accentuated AMPK in TGF- $\beta$ 1-Treated Keloid Fibroblasts**

TGF- $\beta$ -induced cellular responses involve the phosphorylation of several signaling pathways, such as phosphorylation of SMAD2, SMAD3, AMPK, and ERK, which were investigated in this study. TGF- $\beta$  significantly increased the levels of p-SMAD2, p-SMAD3, p-AMPK, and p-ERK. ADP355 (10  $\mu$ g/mL) significantly inhibited the TGF- $\beta$ -induced phosphorylation of SMAD3 and ERK and amplified p-AMPK phosphorylation (Figure 4). However, there was no significant difference observed in the phosphorylation of SMAD2.

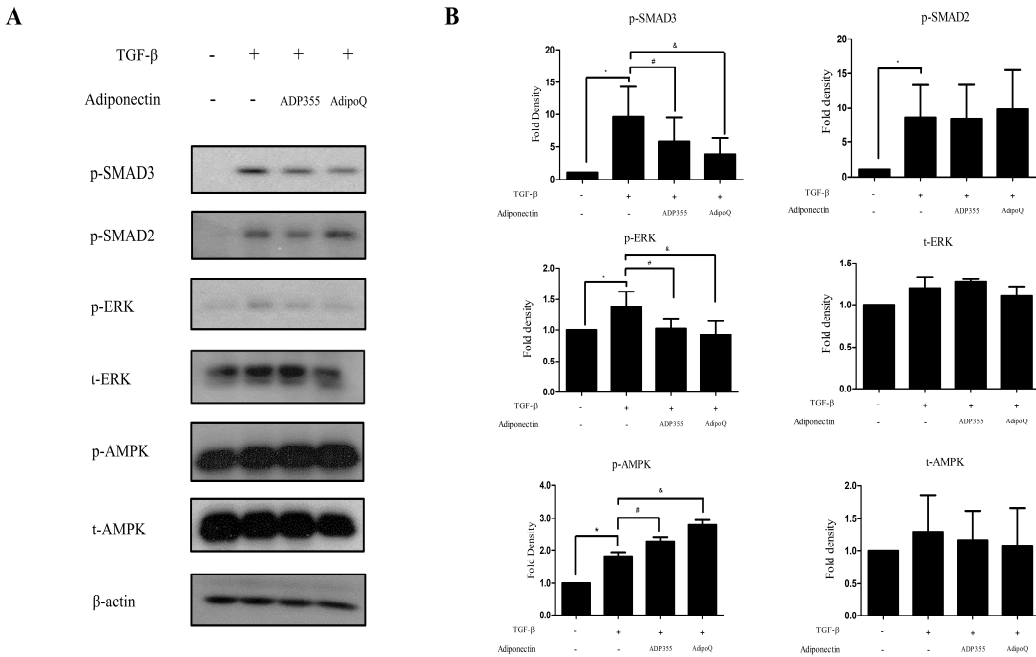


**Figure 4. Effect of ADP355 on the TGF- $\beta$ 1-induced downstream pathways.**

(A) Western blot analysis results. TGF- $\beta$ 1-induced increases in phosphorylation of SMAD2, SMAD3, ERK, and AMPK. Treatment with ADP355 (10  $\mu$ g/mL) and adiponectin recombinant, AdipoQ (10  $\mu$ g/mL), reversed TGF- $\beta$ 1-induced phosphorylation of SMAD3 and ERK and accentuated phosphorylation of AMPK. (B) Quantification of western blot results (\*  $p < 0.05$ , control vs. TGF- $\beta$ 1, #  $p < 0.05$ , TGF- $\beta$ 1 vs. TGF- $\beta$ 1 + ADP355, and TGF- $\beta$ 1 vs. TGF- $\beta$ 1 + AdipoQ). The data are expressed as mean  $\pm$  SD. Representative data are shown from three independent experiments.

## **Knockdown of AdipoR1 Attenuated the Inhibitory Effect of ADP355 on TGF- $\beta$ -Induced Fibrosis**

Adiponectin Receptor 1 (AdipoR1) has been shown to substantially contribute to the ADP355-induced antifibrotic effect, as well as adiponectin recombinant-mediated pathways in keloids<sup>8,13</sup>. Therefore, we used siRNA targeting AdipoR1 to determine whether the antifibrotic effect of ADP355 is reversed by the knockdown of AdipoR1. Specific knockdown of AdipoR1 was confirmed through qRT-PCR expression of AdipoR1, relative to negative-control siRNA (Figure 5A). We confirmed that knockdown of AdipoR1 reversed the attenuation of procollagen expression on ADP355 and AdipoQ-treated TGF- $\beta$ -induced fibrosis (Figure 5B, siRNA+ vs. siRNA-,  $p < 0.05$ ).

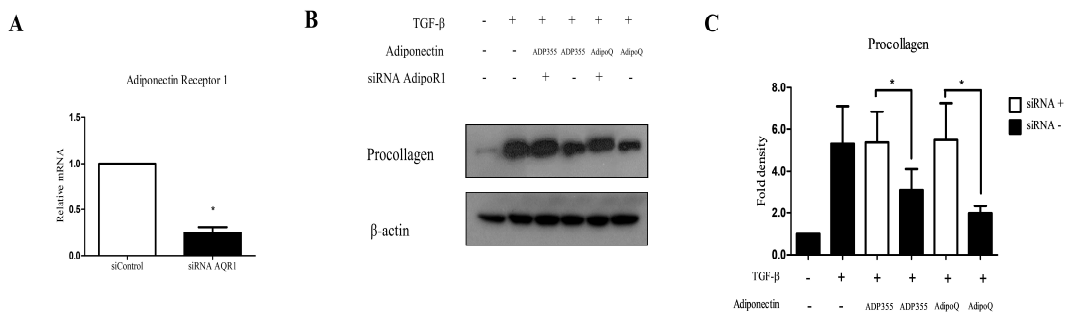


**Figure 5. Knockdown of adiponectin receptor 1 (AdipoR1) reversed the ADP355 attenuation of TGF- $\beta$ 1-induced collagen expression.**

Treatment of ADP355 (5 and 10  $\mu$ g/mL) and adiponectin recombinant, AdipoQ (10  $\mu$ g/mL), simultaneously with TGF- $\beta$ 1 10  $\mu$ g/mL of ADP355 and AdipoQ, attenuated TGF- $\beta$ 1-induced procollagen expression. (A) The effect of adiponectin receptor knockdown was compared with that of a negative control siRNA. (B) Western blot analysis results. Knockdown of AdipoR1 reversed the procollagen expression attenuation by ADP355 and AdipoQ. (C) Quantification of western blot results (\*  $p < 0.05$ , siRNA(+) TGF-  $\beta$ 1 + ADP355 vs siRNA(-) TGF-  $\beta$ 1 + ADP355, siRNA(+) TGF-  $\beta$ 1 + AdipoQ vs siRNA(-) TGF-  $\beta$ 1 + AdipoQ). The data are expressed as mean  $\pm$  SD. Representative data are shown from three independent experiments.

## **Intralesional Injection of ADP355 Reduced the Size and Procollagen Expression of Xenotransplanted Keloid Tissue**

To evaluate the effect of ADP355 in keloid animal models, we implanted keloid tissues excised from patients onto the backs of mice. Following six intralesional injections over 2 weeks (thrice/week), the grafts were excised (Figure 6A). The weight of ADP355-treated lesions were significantly lower than those of the vehicle-treated mice ( $p < 0.05$ , Figure 6B). Western blot analysis showed that procollagen expression was significantly reduced, while expression of p-AMPK was increased, following treatment with ADP355 and AdipoQ ( $p < 0.05$ , Figure 6C).

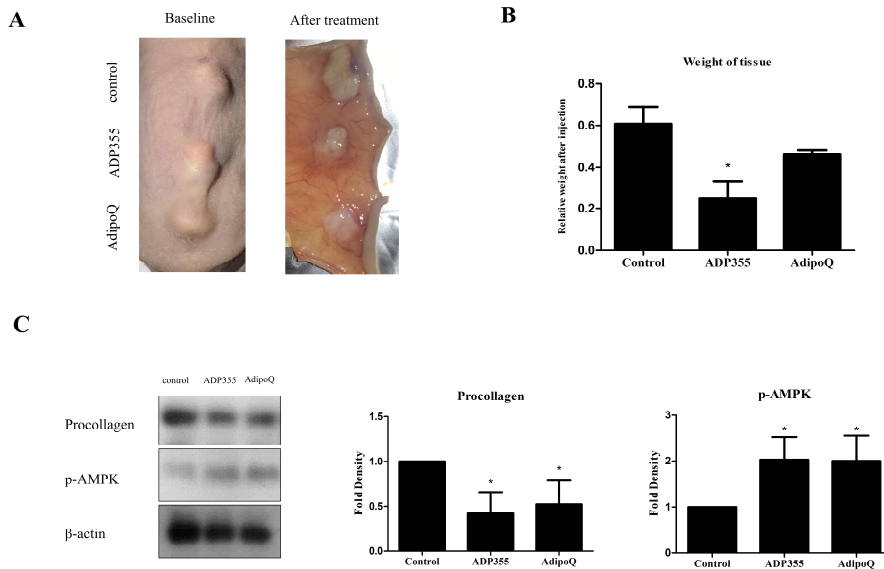


**Figure 6. Intralesional Injection of ADP355 Reduced the Size and Procollagen Expression of Xenotransplanted Keloid Tissue.**

(A) Macroscopic examination of xenotransplanted tissue on the back of athymic nude mice before and after treatment. (B) Weight of xenografted keloid tissues after intralesional injection of ADP355 and AdipoQ. The weight of the tissues was normalized to the baseline weight, and the weight of adiponectin-treated tissue was compared to that of control. ADP355-treated lesions showed a significant weight reduction (\*  $p < 0.05$ ). (C) Procollagen protein expression was significantly reduced while p-AMPK expression increased following treatment with ADP355 and AdipoQ (\*  $p < 0.05$ ). The data are expressed as mean  $\pm$  SD. Representative data are shown from three independent experiments.

## DISCUSSION

Keloid formation is the consequence of the pathologic wound healing process, which involves complex regulatory pathways<sup>20</sup>. Dysregulation of TGF- $\beta$  has been shown to play a prominent role in determining the outcome of keloid formation by upregulation of collagen gene expression<sup>21,22</sup>. Counteracting or blocking the effect of TGF- $\beta$  can reduce the burden of pathological scarring.<sup>23</sup> Inhibition of TGF- $\beta$ /Smad and MAPK/ERK signaling has been shown to counteract TGF- $\beta$ -induced keloid fibroblast proliferation, migration, and invasion, and to simultaneously reduce collagen production<sup>24</sup>.

Adiponectin is an adipokine that is predominantly secreted by the adipose tissue and exerts a multifunctional effect through interaction with cell-surface adiponectin receptors (AdipoRs). It plays a role in multiple organs including the liver, kidney, pancreas, and muscle. Adiponectin reportedly attenuates tissue fibrosis in the liver and kidney<sup>25</sup>. It has also been reported to be involved in the pathogenesis of keloids by influencing cell proliferation and migration and by inducing the overproduction of ECM in keloid fibroblasts<sup>13</sup>. However, its extremely insoluble C-terminal globular domain and large peptide fragments hinder the development of whole adiponectin protein as a drug or for use in other treatment modalities<sup>8</sup>. In this regard, adiponectin-based short peptide agonists may be used as potential alternative therapeutic agents. ADP355 is a 10-amino acid-long peptide that has been reported to have an antitumor effect in breast cancer, an antifibrotic effect on the liver, and to cause partial attenuation of protease inhibitor-induced cognitive impairment and brain injury<sup>8,15,24</sup>. It has also been shown to elicits potent anti-fibrotic effect in normal and systemic sclerosis skin fibroblast in vitro and prevents and reverses skin fibrosis in mice<sup>17</sup>.

Several studies have demonstrated promising application of synthetic peptides for the inhibition and reduction of scarring<sup>26-28</sup>. In a multiple randomized controlled

trial, the effect of aCT1, a transmembrane protein Cx43-mimicking peptide, was investigated. The peptide improved overall scar thickness and pigmentation<sup>27</sup>. Most recently, growth hormone-releasing peptide 6 (GHRP6) has been shown to modulate the expression of several proteins that have been implicated in keloid formation<sup>26</sup>.

In this experiment, we explored the effect of an adiponectin-based receptor agonist, ADP355, on TGF- $\beta$ 1-induced fibrosis of keloid fibroblasts. As AMPK inhibits TGF- $\beta$ -induced transcription downstream of SMAD3 COOH-terminal phosphorylation and nuclear translocation<sup>29</sup>, its amplification can antagonize TGF- $\beta$ 1-induced collagen production. In this study, both adiponectin and ADP355 significantly upregulated the phosphorylation of AMPK in keloid fibroblasts, which, in turn, resulted in a reduction of TGF- $\beta$ 1-induced procollagen expression. ERK MAP kinases phosphorylate receptor-activated SMADS and regulate their nuclear translocation<sup>30</sup>, and the inhibition of TGF- $\beta$ /Smad and MAPK/ERK signaling pathways can antagonize collagen production<sup>24</sup>. Our results revealed that both adiponectin and ADP355 inhibited the TGF- $\beta$ 1-induced phosphorylation of SMAD3 and ERK. Phan et al has demonstrated that SMAD3 was overexpressed in keloid fibroblast compared to normal fibroblast suggesting its role in keloid pathogenesis.<sup>31,32</sup> Knockdown of SMAD3 expression in keloid fibroblast has been shown to reduce ECM deposition and attenuate process of fibrosis in keloid.<sup>32</sup>

In addition, we showed that knockdown of AdipoR1 reversed the antifibrotic effect of both ADP355 and AdipoQ. Collectively, ADP355 reduced the effect of TGF- $\beta$ 1-induced procollagen type 1 expression by attenuating phosphorylation of SMAD3 and ERK signaling and amplifying the p-AMPK pathway through AdipoR1.

Keloids are unique to humans. The differences in skin physiology and models of healing contributes to challenges in modeling keloids in laboratory animals.<sup>33,34</sup> Direct xenografting of keloid tissue into athymic nude mice is one of the most representative approaches for the study of keloid tissue<sup>33</sup>. This approach allows the

observation of human tissue in an *ex vivo* environment by preserving complex human cell–cell interactions in both dermis and epidermis, while limiting the impact of environmental factors <sup>33</sup>. Our results show that the intralesional injections of ADP355 significantly reduced procollagen expression and amplified phosphorylation of AMPK. In line with these results, the weight of ADP355-treated keloid tissue reduced significantly in comparison to that of control tissue.

In conclusion, our study demonstrated the antifibrotic effect of ADP355 in keloid fibroblasts and xenografted keloid tissue in mice. These results suggest a possible therapeutic application of ADP355 in keloid treatment.

## **CHAPTER 2**

### **Dasatinib attenuates fibrosis in keloids by decreasing senescent cell burden**

## BACKGROUND

Cellular senescence, a state in which cell undergoes an arrest of cell cycle induced by cellular stress, has recently been suggested to involve ageing and contribute to some age-related diseases such as cancers, atherosclerosis, and osteoarthritis.<sup>35</sup> Therefore, there have been investigation to alleviate the diseases through selective removal of senescent cells. Senolysis, a therapeutic strategy to induce selective elimination of senescent cells or the detrimental component of the SASP (senescence-associated secretory phenotype). So far, several drugs, including dasatinib, quercetin, navitoclax, and 17-DMAG have shown their selective effect on senescence cells, as senolytics.<sup>36</sup> In patient with systemic sclerosis associated interstitial lung disease, dasatinib showed clinical improvement with decreased expression of SASP and other senescence-related genes, suggesting the role of cellular senescence in fibrotic diseases.<sup>37,38</sup> Moreover, dasatinib plus quercetin has been shown to alleviate physical dysfunction in idiopathic pulmonary fibrosis (IPF) in a human open-label trial.<sup>39,40</sup>

To our knowledge, the role of senescent cells in keloid are largely unknown. Therefore, we performed this study to investigate whether senescent cells are increased in keloids and further to explore the effect of dasatinib as a senolytic drug in keloids.

## **MATERIALS AND METHODS**

### **Ethics statement**

The study protocols were approved by the institutional research board of Seoul National University Hospital (IRB No. C-1912-135-1090), and written informed consent was obtained from all subjects. All experimental procedures using human tissues were conducted according to the principles described in the Declaration of Helsinki. The animal study was approved by the Institutional Animal Care and Use Committee (IACUC) at Seoul National University Hospital (IACUC No. 20-0016-S1A0) and all the methods were performed in accordance with the relevant guidelines and regulations.

### **Keloid biopsy from patient**

After obtaining the informed consent from patients with keloid, the tissues were acquired from keloid removal surgery. They were used to isolate the dermal fibroblast cell line as well as frozen sectioning. The biopsied specimen was divided into two group, lesional and perilesional (macroscopically normal skin adjacent to the lesion).

### **Isolation of keloid dermal fibroblast primary cell culture**

For primary cell culture of dermal fibroblasts, human dermal fibroblasts were isolated by mechanical and enzymatic digestion using previously described protocol. Cells were cultured in Dulbecco's modified Eagle's medium (DMEM, Welgene (Gyeongsan) with penicillin/streptomycin (Life Technologies), and 10% FBS (GE Healthcare Life Sciences, Logan, UT, USA) in a humidified 5% CO<sub>2</sub> atmosphere at 37 C. Only cultured cells at the passage between 1 – 4 were used for the following experiments.

## **Dasatinib treatment**

Cells were cultured to 60% confluence and were starved for 24 hours and, then, treated with either dasatinib or PBS for 24 hours. Cells were treated with dasatinib with varying concentration (1 ng/ml, 5 ng/ml, 10 ng/ml).

## **Senescence-associated $\beta$ -galactosidase analysis**

Upon reaching 40% confluency, senescence associated  $\beta$ -galactosidase activity was measured following manufacturer's instructions using a senescence detection kit (Cell signaling). After 24 hours, the number of positive cells were quantified.

## **RNA and protein extraction**

mRNA and protein were extracted from a snap frozen tissue sample comprised of either keloid or the perilesional tissue. Crushed tissue were lysed with TRIzol method according to manufacturer's protocol consecutively for both RNA and protein analysis.

## **qRT-PCR**

Total RNA (1  $\mu$ g) was used in a 20  $\mu$ l reaction for first-strand cDNA synthesis using First Strand cDNA Synthesis Kit (Thermo Fisher Scientific, MA, USA), according to the manufacturer's protocol. cDNA was subjected to amplification reactions using a 7500 Real-time PCR System (Thermo Fisher Scientific, MA, USA) and SYBR *Premix Ex Taq*, Perfect Real-time (Takara Bio, Japan), according to the manufacturer's protocol, with the following primer pairs: 36B4, p16 and procollagen. PCR thermocycling conditions were as follows: 50°C

for 2 min and 95°C for 2 min, followed by 40 cycles of 95°C for 15 seconds and 60°C for 1 min. Relative mRNA expression levels were normalized to 36B4 and relative expression levels of the target gene were calculated using the  $2^{-\Delta\Delta C_q}$  method. Each experiment was repeated three times.

<b>Gene</b>	<b>Forward Primer</b>	<b>Reverse Primer</b>
P16	CAA CGC ACC GAA TAG TTA CG	CAG CTC CTC AGC CAG GTC
Procollagen	CTC GAG GTG GAC ACC ACC CT	CAG CTG GAT GGC CAC ATC GG
36B4	TGG GCT CCA AGC AGA TGC	GGC TTC GCT GGC TCC CAC

Table 2. Primer sequences for qRT-PCR

### **Western Blot Analysis**

Cells were washed with ice-cold PBS, and lysed with RIPA Lysis Buffer (Millipore) mixed with protease inhibitor mixture (Roche) and phosphatase inhibitor mixture (Sigma-Aldrich). Cell lysates were centrifuged at 13,500 x g at 4°C for 15 minutes, and supernatants were collected. The total extract protein concentration was quantified using a Bicinchoninic Acid Assay reagent (Sigma-Aldrich). Equal amount of proteins was separated by sodium dodecyl sulphate polyacrylamide gel electrophoresis, transferred to polyvinylidene difluoride membranes (Roche). Membrane was blocked with 5% skim milk diluted in Tris-buffered saline containing 0.1% Tween-20, and then were incubated with primary antibodies, such mouse anti-β-actin (Santa Cruz), mouse anti-procollagen (clone SP1.D8, Developmental Studies Hybridoma Bank), rabbit anti-p16 (Abcam, USA) overnight. β-actin was used as a loading control. The membranes were washed and incubated with mouse polyclonal antibody (Genetex, CA, USA) against β-actin, procollagen, rabbit

polyclonal antibody (Genetex, CA, USA) against p16 were given. Immunoreactive bands were visualized using the Enhanced Chemiluminescence Detection System (Thermo Fisher Scientific, MA, USA). Band density was measured with Image J software version 1.51w (National Institutes of Health). Protein expression was normalized to  $\beta$ -actin.

### **Cell Proliferation Assay**

Cells were seeded at a 6 well-plate. Cell were cultured to 60% confluence and were starved for another 24 hours in serum-free DMEM and treated with Dasatinib for 24 hours. Cell viability was tested Ezy-cytox cell viability assay kit (Daeil Bio, Suwon, South Korea) according to manufacturer's instructions. Ezy-cytox reagent was added to each well and incubated for 1 hour and moved to 96-well plate. The absorbance of collected media was determined using spectrophotometric using a microplate reader (Molecular Devices) at 450/650nm.

### **Xenotransplantation of human keloid tissue**

Keloid tissues were acquired from patients with keloid during surgical excision. For xenotransplantation, donor tissues were prepared using a 5mm punch (weight range, 0.09gr – 0.1gr) and preserved in normal saline. Female athymic nude BALB/c mice (age six weeks) were anesthetized with isoflurane, human keloid tissues were transplanted on the recipient site, which was prepared using 5mm punch on each side of the back. Transplantation was done within 2 hours from the acquisition of keloid tissue from patients. 15<sup>th</sup> days after transplantation, the tissue has completely healed and were assigned for intralesional injection with either vehicle (PBS) or dasatinib (10uM) for two weeks (3 times/week). Seven days following the final treatment, the lesions were obtained for further analysis.

## **Immunohistochemical staining**

Tissues from both patients and xenotransplantation mice were fixated on 4% paraformaldehyde solution overnight in 4°C. The tissue block is embedded in paraffin then cut in approximately 5µM using a microtome and affixed onto the slide. Slides were deparaffinized and rehydrated with series of xylene and ethanol solution. Antigen retrieval with Tri-sodium citrate (0.1M sodium citrate, 0.05% Tween 20 pH 6.0) in a high pressure cooker for 30 minutes. Slides were incubated with rabbit anti-p16 (ab54210, Abcam, USA). The primary antibody was washed with PBS and incubated with complementary rabbit secondary antibody for 1 hour. The color was developed using liquid AEC substrate Kit (GBI Labs, WA, USA). The slides were mounted and observed under microscope. The number of p16 positive cells from three field of each sample were quantified manually by three researchers and represented as mean value (SD). To observe the thickness of the procollagen, the tissue section was stained with Hematoxylin and Eosin and Masson' Trichome.

For immunofluorescence staining, the tissue section were incubated with rabbit anti-p16 (ab5421, Abcam). The primary antibody was washed with PBS and incubated with fluorescent-tagged secondary antibody anti-rabbit Alexa Fluor 488 (Invitrogen, Life Technologies, Inc., Carlsbad, CA) antibody for 1 hour at room temperature. The nuclei were counterstaining with DAPI staining. Sections were mounted on slides using Immu-Mount (Thermo Fisher Scientific). Fluorescent image were acquired using the Leica TCS SP8 Microscope.

## **Statistical analysis**

The results of at least three independent representative experiments with each of the data represented as mean values (SD). A Mann-Whitney U test was used to compare medians between two independent groups and Kruskal-Wallis test was used for comparisons of median values among three or more groups, followed by post-hoc testing using Mann-Whitney U tests with a Bonferroni-adjusted alpha level

with SPSS 23.0 software (IBM Co., Armonk, NY, USA) and p values of  $< 0.05$  were considered statistically significant.

## RESULTS

### Senescence associated- $\beta$ -galactosidase positive cells are increased in keloid lesion

First, we compared the presence of senescent fibroblast on lesional and perilesional tissue using senescence-associated  $\beta$ -galactosidase (SA-  $\beta$ -galactosidase) analysis on primary cell culture. Quantitative analysis of cultured fibroblasts demonstrated that the number of SA- $\beta$ -galactosidase positive cells was significantly higher in the lesional fibroblast compared to those in the perilesional fibroblasts ( $p < 0.05$ , Figure 7).

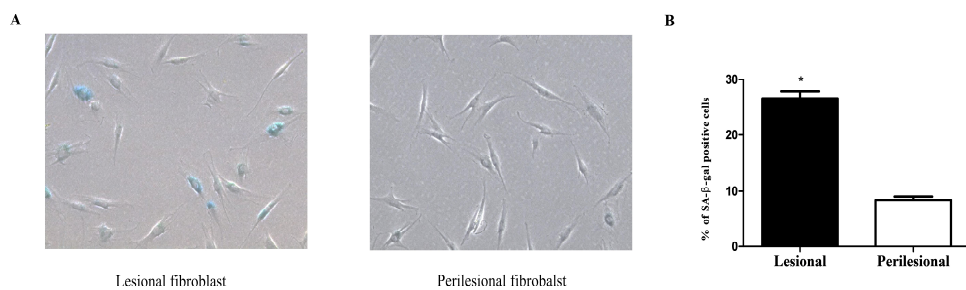


**Figure 7. SA- $\beta$ -galactosidase activity analysis on primary cultured fibroblast of keloid patients.**

(A) SA- $\beta$ -galactosidase positive fibroblasts between keloid lesion and perilesional skin. (B) Quantification of number of SA- $\beta$ -galactosidase positive fibroblasts between keloid lesion and perilesional skin. The data are expressed as mean  $\pm$  SD. Representative data are shown from six independent experiments ( $p < 0.05$ )

## p16 expression was increased in Keloid fibroblasts

To confirm our previous finding, we investigated the expression of p16 on lesional and perilesional tissue. Compared to perilesional skin, keloid lesion showed significantly increased protein expression of p16 as well as procollagen (Figure 8A). In addition, increased expression of p16 was also revealed by qRT-PCR and IHC (Figure 8B-D).

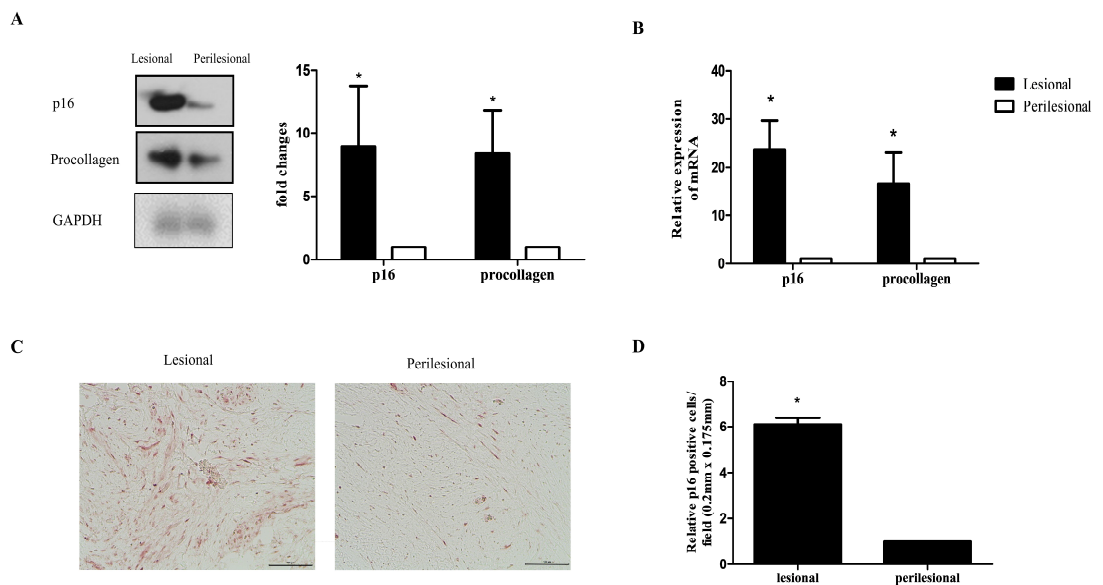


### Figure 8. Expression of p16 in keloid lesion.

(A) Western blot showing increased expression of p16 and procollagen expression in keloid lesion compared to those in the perilesional skin. ( $p < 0.05$ ) (B) mRNA expression of p16 and procollagen in keloid tissue and perilesional skin. ( $p < 0.05$ ) (C) Representative image of immunostaining with anti-p16 antibody (Scale bars; 100 μm) (D) Relative changes on number of p16-expressing cells between lesional and perilesional tissue ( $p < 0.05$ ). The data are expressed as mean  $\pm$  SD. Representative data are shown from three independent experiments.

### **Dasatinib exerts selective elimination of p16-positive cells and reduced procollagen expression.**

To evaluate the effect of dasatinib on cultured keloid cells, several doses of dasatinib (1nM – 1uM) were treated. Cell viability and number of senescent cell were evaluated by MTT assay and SA- $\beta$ -Gal assay, respectively. Although dasatinib did not affect cultured cells from perilesional skin up to a dose of 10 nM, cultured cells from keloid lesion underwent significant cell death by treatment with 1nM of dasatinib. When we analyzed the percentage of  $\beta$ -galactosidase-positive cells, the data showed a significant decrease by treatment start from 1nM of dasatinib in cultured cells from keloid lesion (Figure 9A). These findings suggested that dasatinib selectively decreased  $\beta$ -galactosidase-positive cells in keloid fibroblasts. Subsequently, the experiment was conducted within the window range from 1nM – 10nM. After 24hrs treatment with dasatinib (1-10 $\mu$ M), dasatinib significantly reduced the protein expression of p16 and procollagen in keloid fibroblasts (Figure, 9B-C).

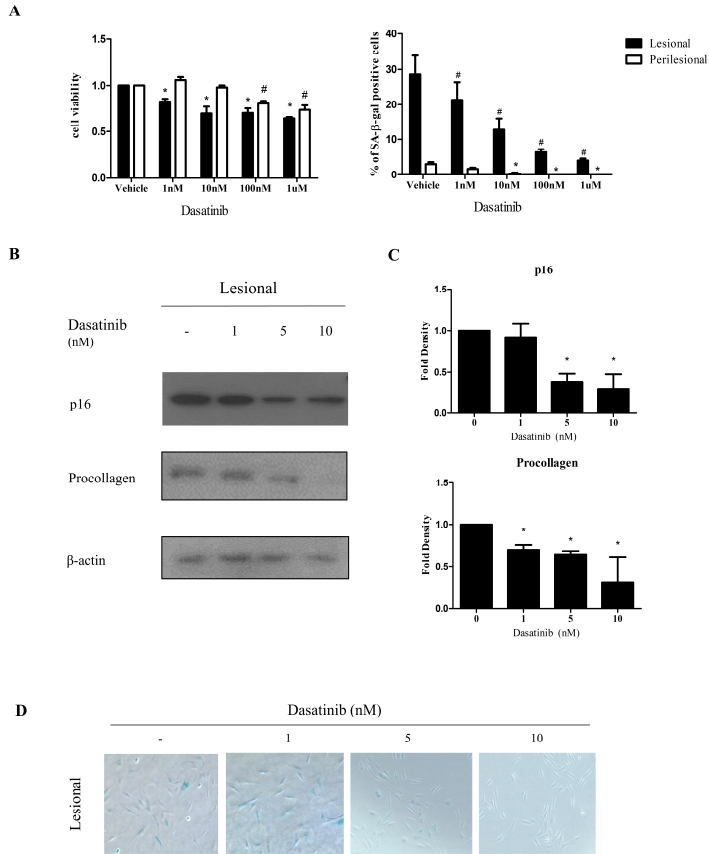


**Figure 9. Effect of dasatinib on cultured keloid fibroblasts.**

(A) Total number of cell and percentage of SA-β-galactosidase positive cells were measured in fibroblasts cultured from either lesional or perilesional tissue after treatment of dasatinib (1nM – 1uM) for 24 hours. (B) Western blot showing both procollagen and p16 expression in lesional fibroblasts treated with either dasatinib. (C) Quantification of western blot results showing reduction of procollagen and p16 expression in concentration-dependent manner ( $p < 0.05$ ). (D) The SA-β-galactosidase staining shows reduction of SA-β-galactosidase in concentration dependent manner (1nM- 10nM). The data are expressed as mean  $\pm$  SD. Representative data are shown from three independent experiments.

### **Intralesional injection of dasatinib reduced the size of xenotransplanted keloid tissue and suppressed the expression of procollagen and p16**

To validate the senolytic effect of dasatinib on keloid in vivo, we implanted the human keloid tissues from patients onto the back of athymic nude BALB/c mice. Following six intralesional injections of dasatinib (10nM) over 2 weeks (thrice/week), the xenograft tissues were extirpated and evaluated (Figure 10A). The weight reduction changes in dasatinib-treated lesions were significantly higher compared to that in the vehicle-treated lesions ( $p < 0.05$ , Figure 10B). Both p16 and procollagen protein expression on dasatinib-treated lesion were significantly lower compared to those in the control (Figure 10C-D). Histopathological analysis showed reduced the collagen bundle thickness in dasatinib-treated tissue in hematoxylin and eosin and Masson's Trichrome staining (Figure 11A). Immunofluorescence staining of p16 cells and quantification of p16-positive cells showed significant reduction of p-16 positive cells on dasatinib-treated lesion ( $p < 0.05$ , Figure 11B).

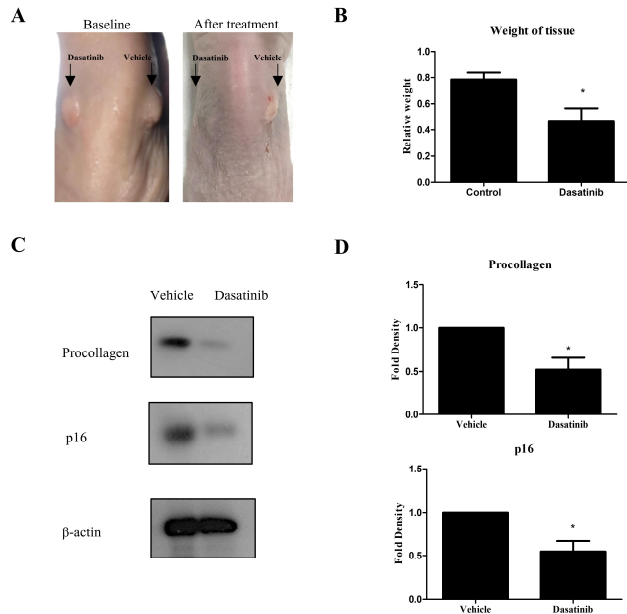


**Figure 10. The effect of dasatinib on xenotransplantation model of keloid.** (A) The macroscopic examination of the dasatinib-treated (right) and the vehicle-treated (left) keloid tissues. (B) The weight changes of the tissue after intralesional treatment of either dasatinib (10nM) or PBS for 2 weeks (3 times/week), ( $p < 0.05$ ). (C) Western blot analysis of procollagen and p16 expression from dasatinib treated lesion and vehicle treated lesion. ( $p < 0.05$ ) (D) Quantification of western blot results. ( $p < 0.05$ ). The data are expressed as mean  $\pm$  SD. Representative data are shown from three independent experiments.

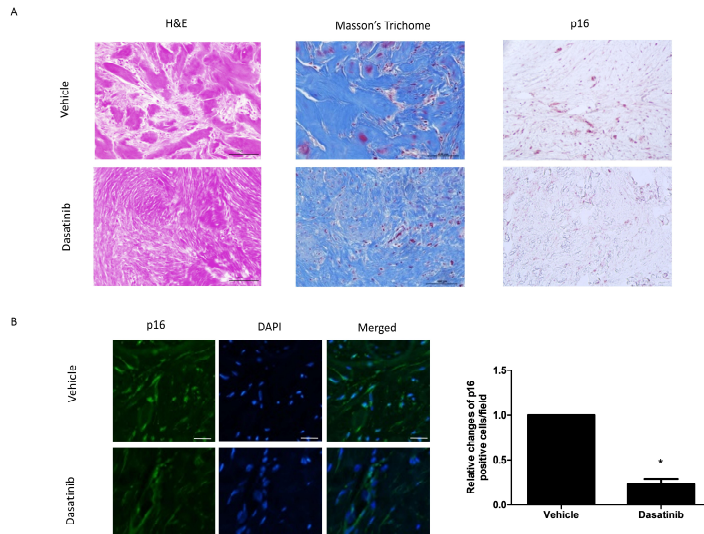


**Figure 11. Histopathological analysis of intralesional Dasatinib on xenotransplantation model of keloid.** (A) Hemotoxylin and Eosin, Masson's Trichome and p16 IHC staining of vehicle- and dasatinib-treated lesion from left-right. (Scale bars, 100  $\mu$ m). (B) Immunofluorescence staining of p16 cells and quantification of p16-positive cells on vehicle-treated and dasatinib-treated lesion (scale bars = 50 $\mu$ m,  $p < 0.05$ ). The data are expressed as mean  $\pm$  SD. Representative data are shown from three independent experiments.

## DISCUSSION

The roles of senescent cells have been assessed in several skin disorders. Nakamura S et al. showed that seborrheic keratosis have increased p16 expression in keratinocytes.<sup>41</sup> Vitiligo, which is considered to be caused mainly by genetic susceptibility and autoimmune, also showed altered signal transduction that induce premature senescence.<sup>42</sup> In addition, production of SASP such as interleukin-6 (IL-6), matrix metallo proteinase-3 (MMP3), cyclooxygenase-2 (Cox-2), insulin-like growth factor-binding protein-3 and 7 (IGFBP3, IGFBP7) are highly expressed in vitiligo melanocytes.<sup>42</sup> Melasma and senile lentigo, which clinically manifested hyperpigmentation, has also been shown to accumulated senescent cells. Senescent fibroblast could both either exacerbate or repress melanogenesis.<sup>43,44</sup> In lesional skin of senile lentigo, biologic roles of stromal-derived factor 1 (SDF1) in senescent fibroblasts led to stimulation of melanogenic process via stromal-epithelial interactions.<sup>45</sup> Senescent fibroblasts are also increased in the lesional skin of idiopathic guttate hypomelanosis (IGH). An increased number of senescent fibroblast contribute to hypopigmentation in IGH by inducing senescence and apoptosis of melanocytes through secretion of SASP factors.<sup>46,47</sup> A rapid accumulation of senescent cells have been found in diabetic mouse skin.<sup>48</sup> Interestingly, in aged and diabetic wounds, there are higher number of senescent cells and production of CXCR2-enriched SASP phenotype that induced profibrotic fibroblast phenotype, such as SERPINE1 and COL1A1.<sup>48</sup> Moreover, the increased expression of p16 was also found in keloid lesion.<sup>49</sup>

<b>Authors, years</b>	<b>Skin disease</b>	<b>Findings</b>	<b>Biologic roles of senescent cells on skin disease</b>
Nakamura S et al <sup>41</sup> , 2003	Seborrheic keratosis	Increased p16 expression in keratinocytes of seborrheic keratosis	Not reported
Belle B et al <sup>42</sup> , 2013	Vitiligo	Increased senescent melanocytes in lesional skin of vitiligo	Increase production of biologically active SASP (IL-6, MMP3, Cox-2, IGFBP3, IGFBP7)
Espósito ACC et al <sup>44</sup> , 2018	Melasma	Increased p38 in the upper dermis of lesional skin	Not reported
Yoon JE et al <sup>45</sup> , 2018	Lentigo	Increased senescent fibroblast in lesional skin	Induces skin pigmentation through repression of stromal-derived factor 1 (SDF1)
Kim JY et al <sup>46</sup> , 2019	Idiopathic guttate hypomelanosis	Increased senescent fibroblast in lesional skin	Induces senescence and apoptosis of melanocyte via SASP from senescent fibroblast
Wilkinson HN et al <sup>48</sup> , 2019	Diabetic wound healing	Increased local senescence in diabetic dermal fibroblast	Excessive CXCR2 and SASP drives upregulation of SERPINE1 and COL1A1

Table 3. Skin diseases associated with cellular senescence

In this experiment, we examined the presence of senescent cells in keloid fibroblasts as well as in the tissues and found increased senescent cells in the keloid lesion. These findings were consistent with previous studies.<sup>49,50</sup> We further found the anti-fibrotic and senolytic effect of dasatinib in the keloid fibroblasts. Dasatinib reduced the expression of procollagen as well as senescent cells burden in keloid in vitro. Moreover, keloid xenopplantation model, in which human keloid tissues were implanted in athymic nude mice, showed that intralesional injection of dasatinib reduced the macroscopic size and weight of xenotransplanted tissue ( $p < 0.05$ ). p16 and procollagen expression were also significantly decreased in dasatinib-treated tissue compared to vehicle. In H&E and Masson Trichome's staining, reduced

collagen bundle thickness was revealed in dasatinib-treated tissue. The expression of p16 positive cell on immunofluorescence staining is also significantly reduced compared to the vehicle-treated lesion in immunofluorescence staining ( $p < 0.05$ ).

In addition to keloid, senescent cells accumulation also plays direct roles in fibrosis and contributing to fibrotic diseases in liver, kidney, and lung.<sup>39,51,52</sup> Therefore, the use of senotherapeutics may be a viable strategy for treatment of a range of fibrotic conditions.<sup>51</sup> An initial clinical evidence that warrant the benefit of senolytics therapy for fibrotic disease such as pulmonary fibrosis and systemic sclerosis related-interstitial lung disease (SSc-ILD) have also been shown.<sup>38,39,53</sup>

Collectively, our results demonstrated the senolytic and anti-fibrotic effect by dasatinib in keloid fibroblasts and xenografted keloid tissue in mice. These findings suggested a possible therapeutic application of senolytic treatment in keloids. A further clinical study by intralesional injection of dasatinib are required to confirm the attenuations of fibrosis in keloid by reducing the senescent cell burden.

## REFERENCES

1. Murray JC. Keloids and hypertrophic scars. *Clinics in dermatology*. 1994;12(1):27-37.
2. Marneros AG, Norris JE, Watanabe S, Reichenberger E, Olsen BR. Genome scans provide evidence for keloid susceptibility loci on chromosomes 2q23 and 7p11. *The Journal of investigative dermatology*. 2004;122(5):1126-1132.
3. Tsai CH, Ogawa R. Keloid research: current status and future directions. *Scars Burn Heal*. 2019;5:2059513119868659.
4. Hsueh WT, Hung KS, Chen YC, et al. Adjuvant Radiotherapy After Keloid Excision: Preliminary Experience in Taiwan. *Annals of plastic surgery*. 2019;82(1S Suppl 1):S39-s44.
5. Seo BF, Jung SN. The Immunomodulatory Effects of Mesenchymal Stem Cells in Prevention or Treatment of Excessive Scars. *Stem cells international*. 2016;2016:6937976.
6. Bijlard E, Kouwenberg CA, Timman R, Hovius SE, Busschbach JJ, Mureau MA. Burden of Keloid Disease: A Cross-sectional Health-related Quality of Life Assessment. *Acta dermato-venereologica*. 2017;97(2):225-229.
7. Gauglitz GG. Current therapeutic approaches for the treatment of keloids. *Aktuelle Dermatologie*. 2011;37(3):75-80.
8. Otvos L, Haspinger E, La Russa F, et al. Design and development of a peptide-based adiponectin receptor agonist for cancer treatment. *BMC Biotechnology*. 2011;11(1):90.
9. Brochu-Gaudreau K, Rehfeldt C, Blouin R, Bordignon V, Murphy BD, Palin MF. Adiponectin action from head to toe. *Endocrine*. 2010;37(1):11-32.
10. Yamauchi T, Kamon J, Minokoshi Y, et al. Adiponectin stimulates glucose utilization and fatty-acid oxidation by activating AMP-activated protein kinase. *Nat Med*. 2002;8(11):1288-1295.
11. Deepa SS, Zhou L, Ryu J, et al. APPL1 mediates adiponectin-induced LKB1 cytosolic localization through the PP2A-PKCzeta signaling pathway. *Mol Endocrinol*. 2011;25(10):1773-1785.
12. Achari AE, Jain SK. Adiponectin, a Therapeutic Target for Obesity, Diabetes, and Endothelial Dysfunction. *Int J Mol Sci*. 2017;18(6):1321.
13. Luo L, Li J, Liu H, et al. Adiponectin Is Involved in Connective Tissue Growth Factor-Induced Proliferation, Migration and Overproduction of the Extracellular Matrix in Keloid Fibroblasts. *Int J Mol Sci*. 2017;18(5).
14. Wu X, Motoshima H, Mahadev K, Stalker TJ, Scalia R, Goldstein BJ. Involvement of AMP-activated protein kinase in glucose uptake stimulated by the globular domain of adiponectin in primary rat adipocytes. *Diabetes*. 2003;52(6):1355-1363.

15. Wang H, Zhang H, Zhang Z, et al. Adiponectin-derived active peptide ADP355 exerts anti-inflammatory and anti-fibrotic activities in thioacetamide-induced liver injury. *Scientific Reports*. 2016;6:19445.
16. Kumar P, Smith T, Rahman K, Thorn NE, Anania FA. Adiponectin agonist ADP355 attenuates CCl4-induced liver fibrosis in mice. *PLoS One*. 2014;9(10):e110405.
17. Marangoni RG, Masui Y, Fang F, et al. Adiponectin is an endogenous anti-fibrotic mediator and therapeutic target. *Sci Rep*. 2017;7(1):4397.
18. Kisiel MA, Klar AS. Isolation and Culture of Human Dermal Fibroblasts. In: Böttcher-Haberzeth S, Biedermann T, eds. *Skin Tissue Engineering: Methods and Protocols*. New York, NY: Springer New York; 2019:71-78.
19. Gassmann M, Grenacher B, Rohde B, Vogel J. Quantifying Western blots: pitfalls of densitometry. *Electrophoresis*. 2009;30(11):1845-1855.
20. Berman B, Maderal A, Raphael B. Keloids and Hypertrophic Scars: Pathophysiology, Classification, and Treatment. *Dermatologic surgery : official publication for American Society for Dermatologic Surgery [et al]*. 2017;43 Suppl 1:S3-s18.
21. Martin P, Dickson MC, Millan FA, Akhurst RJ. Rapid induction and clearance of TGF beta 1 is an early response to wounding in the mouse embryo. *Dev Genet*. 1993;14(3):225-238.
22. Babu M, Diegelmann R, Oliver N. Keloid fibroblasts exhibit an altered response to TGF-beta. *The Journal of investigative dermatology*. 1992;99(5):650-655.
23. Jagadeesan J, Bayat A. Transforming growth factor beta (TGFβ) and keloid disease. *International Journal of Surgery*. 2007;5(4):278-285.
24. Wang W, Qu M, Xu L, et al. Sorafenib exerts an anti-keloid activity by antagonizing TGF-beta/Smad and MAPK/ERK signaling pathways. *J Mol Med (Berl)*. 2016;94(10):1181-1194.
25. Ruan C-C, Li Y, Ma Y, Zhu D-L, Gao P-J. YIA 03-02 ADIPONECTIN-MEDIATED EPITHELIAL AUTOPHAGY ATTENUATES HYPERTENSIVE RENAL FIBROSIS. *Journal of Hypertension*. 2016;34:e204.
26. Fernandez-Mayola M, Betancourt L, Molina-Kautzman A, et al. Growth hormone-releasing peptide 6 prevents cutaneous hypertrophic scarring: early mechanistic data from a proteome study. *Int Wound J*. 2018;15(4):538-546.
27. Grek CL, Montgomery J, Sharma M, et al. A Multicenter Randomized Controlled Trial Evaluating a Cx43-Mimetic Peptide in Cutaneous Scarring. *The Journal of investigative dermatology*. 2017;137(3):620-630.
28. Zhao BM, Hoffmann FM. Inhibition of transforming growth factor-beta1-induced signaling and epithelial-to-mesenchymal transition by the Smad-binding peptide aptamer Trx-SARA. *Mol Biol Cell*. 2006;17(9):3819-3831.

29. Mishra R, Cool BL, Laderoute KR, Foretz M, Viollet B, Simonson MS. AMP-activated protein kinase inhibits transforming growth factor-beta-induced Smad3-dependent transcription and myofibroblast transdifferentiation. *The Journal of biological chemistry*. 2008;283(16):10461-10469.
30. Kretzschmar M, Doody J, Timokhina I, Massagué J. A mechanism of repression of TGFbeta/ Smad signaling by oncogenic Ras. *Genes Dev*. 1999;13(7):804-816.
31. Phan TT, Lim IJ, Aalami O, et al. Smad3 signalling plays an important role in keloid pathogenesis via epithelial-mesenchymal interactions. *J Pathol*. 2005;207(2):232-242.
32. Wang Z, Gao Z, Shi Y, et al. Inhibition of Smad3 expression decreases collagen synthesis in keloid disease fibroblasts. *Journal of plastic, reconstructive & aesthetic surgery : JPRAS*. 2007;60(11):1193-1199.
33. Marttala J, Andrews JP, Rosenbloom J, Uitto J. Keloids: Animal models and pathologic equivalents to study tissue fibrosis. *Matrix Biology*. 2016;51:47-54.
34. Supp DM. Animal Models for Studies of Keloid Scarring. *Adv Wound Care (New Rochelle)*. 2019;8(2):77-89.
35. Childs BG, Gluscevic M, Baker DJ, et al. Senescent cells: an emerging target for diseases of ageing. *Nature Reviews Drug Discovery*. 2017;16:718.
36. Kirkland JL, Tchkonja T, Zhu Y, Niedernhofer LJ, Robbins PD. The Clinical Potential of Senolytic Drugs. *J Am Geriatr Soc*. 2017;65(10):2297-2301.
37. Martyanov V, Kim GJ, Hayes W, et al. Novel lung imaging biomarkers and skin gene expression subsetting in dasatinib treatment of systemic sclerosis-associated interstitial lung disease. *PLoS One*. 2017;12(11):e0187580.
38. Martyanov V, Whitfield ML, Varga J. Senescence signature in skin biopsies from systemic sclerosis patients treated with senolytic therapy: potential predictor of clinical response? *Arthritis Rheumatol*. 2019.
39. Justice JN, Nambiar AM, Tchkonja T, et al. Senolytics in idiopathic pulmonary fibrosis: Results from a first-in-human, open-label, pilot study. *EBioMedicine*. 2019;40:554-563.
40. Toutfaire M, Bauwens E, Debacq-Chainiaux F. The impact of cellular senescence in skin ageing: A notion of mosaic and therapeutic strategies. *Biochemical Pharmacology*. 2017;142:1-12.
41. Nakamura S, Nishioka K. Enhanced expression of p16 in seborrheic keratosis; a lesion of accumulated senescent epidermal cells in G1 arrest. *The British journal of dermatology*. 2003;149(3):560-565.
42. Bellei B, Pitisci A, Ottaviani M, et al. Vitiligo: A Possible Model of Degenerative Diseases. *PLOS ONE*. 2013;8(3):e59782.

43. Bellei B, Picardo M. Premature cell senescence in human skin: Dual face in chronic acquired pigmentary disorders. *Ageing Research Reviews*. 2020;57:100981.
44. Espósito ACC, Brianezi G, de Souza NP, Miot LDB, Marques MEA, Miot HA. Exploring pathways for sustained melanogenesis in facial melasma: an immunofluorescence study. *Int J Cosmet Sci*. 2018;40(4):420-424.
45. Yoon JE, Kim Y, Kwon S, et al. Senescent fibroblasts drive ageing pigmentation: A potential therapeutic target for senile lentigo. *Theranostics*. 2018;8(17):4620-4632.
46. Kim JY, Lee SH, Ahn Y, et al. Role of senescent fibroblasts in the development of idiopathic guttate hypomelanosis. *The British journal of dermatology*. 2020;182(6):1481-1482.
47. Kim JY, Lee SH, Ahn Y, et al. Role of senescent fibroblasts in the development of idiopathic guttate hypomelanosis. *The British journal of dermatology*. 2019;10.1111/bjd.18801.
48. Wilkinson HN, Clowes C, Banyard KL, Matteucci P, Mace KA, Hardman MJ. Elevated Local Senescence in Diabetic Wound Healing Is Linked to Pathological Repair via CXCR2. *Journal of Investigative Dermatology*. 2019;139(5):1171-1181.e1176.
49. Limandjaja GC, Belien JM, Scheper RJ, Niessen FB, Gibbs S. Hypertrophic and keloid scars fail to progress from the CD34(-) / $\alpha$ -smooth muscle actin ( $\alpha$ -SMA)(+) immature scar phenotype and show gradient differences in  $\alpha$ -SMA and p16 expression. *Br J Dermatol*. 2019;10.1111/bjd.18219.
50. Varmeh S, Egia A, McGruther D, Tahan SR, Bayat A, Pandolfi PP. Cellular senescence as a possible mechanism for halting progression of keloid lesions. *Genes Cancer*. 2011;2(11):1061-1066.
51. Schafer MJ, Haak AJ, Tschumperlin DJ, LeBrasseur NK. Targeting Senescent Cells in Fibrosis: Pathology, Paradox, and Practical Considerations. *Curr Rheumatol Rep*. 2018;20(1):3-3.
52. Xiao M, Chen W, Wang C, et al. Senescence and cell death in chronic liver injury: roles and mechanisms underlying hepatocarcinogenesis. *Oncotarget*. 2017;9(9):8772-8784.
53. Campisi J, d'Adda di Fagagna F. Cellular senescence: when bad things happen to good cells. *Nature Reviews Molecular Cell Biology*. 2007;8(9):729-740.

## 국문초록

### 아디포넥틴 유래의 펩타이드와 다사티닙의 켈로이드 억제효과

서울대학교 의과대학 의학과 피부과학 전공

Claudia Christin Darmawan

켈로이드는 피부가 손상된 후 발생하는 상처 치유과정에서, 병리적으로 피부 섬유아세포가 과증식되어 발생하는 피부 질환이다. 이 질환은 피부 조직에 심한 손상을 입었을 때 뿐만 아니라 경미한 손상 후에도 발생할 가능성이 있다고 알려져 있다. 켈로이드는 대부분 장기간 지속되고 자발적으로 회복되지 않고, 환자의 삶의 질에 신체적 및 심리적으로 큰 영향을 미친다. 하지만 이 질환의 병인은 현재까지 명확하게 밝혀지지 않았으며, 이 질환에 시행되고 있는 다양한 외과적 치료 및 약물적 치료는 효과는 제한적이라, 새로운 치료법의 개발에 대한 연구가 필요하다. .

본 연구의 챕터 1 장에서는 켈로이드 병변에서 아디포넥틴 유래 펩타이드의 효과를 관찰하였다. 인간 켈로이드 병변 유래 섬유아세포 및 마우스에 이식된 인간 켈로이드 조직을 사용하였다. 먼저, 켈로이드 제거 수술을 받는 환자에서 켈로이드 조직을 획득하였다. 획득한 조직을 1 차 배양하여 섬유아세포를 획득하고, 이 세포에 아디포넥틴 유래 펩타이드를 처리하여 TGF- $\beta$ 1 에 의한 섬유화 효과를 평가 하였다. 또한, 켈로이드 조직을

무 흥선 누드 마우스의 등에 이식하고, 이식된 켈로이드 조직에 아디포넥틴 유래 펩타이드를 주입하여, 펩타이드의 항 섬유화 효과를 확인하였다. 결과적으로, 아디포넥틴 유래 펩타이드는 켈로이드 유래 섬유아세포에서 TGF- $\beta$ 1 에 의해 유도된 프로콜라겐 타입 1 (procollagen type 1)의 유전자 및 단백질 발현을 유의하게 감소시켰다 ( $p < 0.05$ ). 이 때, 아디포넥틴 수용체 1 (Adiponectin receptor 1) siRNA 를 이용하여 아디포넥틴 수용체 1 를 억제하면, 아디포넥틴 유래 펩타이드에 의해 감소한 TGF- $\beta$ 1 유도 프로콜라겐 타입 1 의 발현이 다시 증가되는 것을 확인하였다 ( $p < 0.05$ ). 또한, 아디포넥틴 유래 펩타이드는 TGF- $\beta$ 1 에 의해 유도된 mothers against decapentaplegic homolog 3 (SMAD3) 및 extracellular signal-regulated kinases (ERK)의 인산화를 억제하고 5' AMP-activated protein kinase (AMPK)의 인산화를 증가 시켰다 ( $p < 0.05$ ). 마우스에 이식된 켈로이드 조직에 아디포넥틴 유래 펩타이드를 주입하면, 대조군을 주입한 조직보다 조직의 총 중량 및 프로콜라겐 발현을 유의하게 감소하는 것을 관찰하였다.

연구의 2 장에서는, 켈로이드 세포에서 노화 (senescent) 섬유아세포의 존재를 조사하였다. 본 연구자는 켈로이드에서 노화성 섬유아세포의 존재를 조사하고, 켈로이드 섬유아세포에서 다사티닙의 세놀라이틱(senolytics) 효과를 평가하였다.  $\beta$ -갈락토시다제 양성 세포 및 p16 발현 세포는 켈로이드 섬유아세포에서 주변 정상 섬유아세포에 비해

더 높았다 ( $p < 0.05$ ). 다사티닙이 노화된 세포의 선택적 사멸 뿐만 아니라 배양된 켈로이드 섬유 아세포에서 프로 콜라겐의 발현 감소를 유도함을 관찰하였다. 또한, 켈로이드의 이중 이식 모델에서 다사티닙의 병변 내 주사가 켈로이드 조직의 총 중량 및 프로콜라겐과 p16 발현을 감소 시켰음을 확인하였다.

저자는 본 연구를 통해 아디포넥틴 기반 펩티드 및 다사티닙의 켈로이드 치료제로서 대안적인 가능성을 보여 주었다.

**주요어** : 켈로이드, 흉터, 아디포넥틴, 펩타이드, 치료, 노화,  
세놀리틱스, 다사티닙

**학 번** : 2017-23763

## ACKNOWLEDGEMENTS

I would like to express my deepest appreciation to my advising professor, Professor Je-Ho Mun, and the chairman of the dermatology department at Seoul National University, Professor Jin-Ho Chung for their continuous support, guidance and help throughout my years of study, research up until this dissertation is completed.

I would also like to thank my committee members, Professor Si-Hyung Lee from the Department of Dermatology at Seoul National University, Professor Sang-Hwa Kim from Department of Plastic and Reconstructive Surgery at Seoul National University and Professor Jee-Woong Choi from department of dermatology at Ajou University for their valuable feedback and time.

I would also like to express my gratitude towards my colleague and friends at Laboratory of Cutaneous Aging Research & Hair Biology. Last but not least, I would like to thank my parents for their endless support throughout my study at Seoul National University. I would not be able to made this accomplishment without all of their support.